한국측량학회지, 제 25권 제 6-1호, pp. 507~516(2007년 12월 31일)

3D Building Reconstruction and Visualization by Clustering Airborne LiDAR Data and Roof Shape Analysis

Dong-Cheon Lee[1] · Hyung-Sup Jung[2] · Jae-Hong Yom[3]

Abstract

Segmentation and organization of the LiDAR (Light Detection and Ranging) data of the Earth's surface are difficult tasks because the captured LiDAR data are composed of irregularly distributed point clouds with lack of semantic information. The reason for this difficulty in processing LiDAR data is that the data provide huge amount of the spatial coordinates without topological and/or relational information among the points. This study introduces LiDAR data segmentation technique by utilizing histograms of the LiDAR height image data and analyzing roof shape for 3D reconstruction and visualization of the buildings. One of the advantages in utilizing LiDAR height image data is no registration required because the LiDAR data are geo-referenced and ortho-projected data. In consequence, measurements on the image provide absolute reference coordinates. The LiDAR image allows measurement of the initial building boundaries to estimate locations of the side walls and to form the planar surfaces which represent approximate building footprints. LiDAR points close to each side wall were grouped together then the least-square planar surface fitting with the segmented point clouds was performed to determine precise location of each wall of an building. Finally, roof shape analysis was performed by accumulated slopes along the profiles of the roof top. However, simulated LiDAR data were used for analyzing roof shape because buildings with various shapes of the roof do not exist in the test area. The proposed approach has been tested on the heavily built-up urban residential area. 3D digital vector map produced by digitizing complied aerial photographs was used to evaluate accuracy of the results. Experimental results show efficiency of the proposed methodology for 3D building reconstruction and large scale digital mapping especially for the urban area.

Keywords : LiDAR, 3D building modeling, Clustering, Roof shape analysis

1. Introduction

Airborne topographic LiDAR systems with capability of cost-effectiveness, geometric accuracy, and rapid data acquisition have an innovative impact on the present surveying and mapping professions. In the mid 1990s, development of the sensor technologies for LiDAR system reached a degree which satisfied the required accuracy for mapping applications. LiDAR technology has received growing attention and has become increasingly common in various fields of application such as forestry, corridor mapping, city and building modeling, damage assessment, emergency response, virtual reality, and game industry due to its inherent advantages of active sensor and rapid spatial data acquisition capability (Flood, 1999; Fowler, 2001; Romano, 2004). Also in the mapping community, LiDAR systems have emerged as a state-of-the-art technology promising its potential for automatic digital mapping. Major tasks in the processing of LiDAR data involve classification, segmentation, and building modeling (Lee and Schenk, 2001; Suveg and Vosselman, 2000; Khoshelham, 2004). Human visual system often successfully groups the spatially distributed points into meaningful objects or features easily by utilizing cognitive and perceptual processing.

LiDAR data mainly consist of 3D coordinates and

1) Corresponding Author · Department of Geoinformation Engineering, Sejong University (E-mail: dclee@sejong.ac.kr)
2) Department of Earth System Sciences, Yonsei University (Email: geohyung@yonsei.ac.kr)
3) Department of Geoinformation Engineering, Sejong University (E-mail: jhyom@sejong.ac.kr)

intensity return of the laser beams. While 3D coordinates provide precise positions directly, intensity return data recording amplitude of the energy reflected from the surface, which provides information about the types of the surface. Semantic information could be extracted by visualizing LiDAR height data (Forlani *et al.*, 2003). Building reconstruction through the combination of LiDAR data and optical imagery is becoming a popular scheme (Chen *et al.*, 2004; Forkuo and King, 2004). Fusion of LiDAR data and imagery would be complementary in various aspects (Schenk and Csathó, 2002). Images enrich LiDAR data by providing semantic information, however, co-registration of the data is required in most cases for successful integration of data from different sensors (Habib *et al.*, 2005; Habib and Schenk, 1999). On the other hand, gray value coded LiDAR data do not require coordinate registration. Therefore, information about building boundaries or corners extracted from the LiDAR image is directly refers to the object space without registration process.

The purpose of this study is to introduce a strategy of LiDAR data segmentation and roof shape analysis for building reconstruction that eventually produces 3D building information for digital vector maps. The initial building side walls were constructed by measuring the corner points on the LiDAR height image. The initial building side walls were then refined through the least-square adjustment with segmented points for each surface. Reconstruction of the complex roof type with LiDAR data is one of the most challenging tasks. Alharthy and Bethel (2004) suggested moving surface method in 3D parameter space to reconstruct complex roofs (Alharthy and Bethel, 2004). Mass and Vosselman (1999) described derivation of house parameters based on the invariant moment method (Maas and Vosselman, 1999).

This study introduces a novel approach to reconstruct complex roof type using the slope accumulation method. Frequent map revision and increased reliability is becoming a major requirement with increased demand for and use of geospatial information especially in present day applications such as web and wireless GIS, telematics and car navigation. The LiDAR technology will provide these requirements with its on-demand rapid mapping capability.

2. Building Detection and LiDAR Point Clustering

LiDAR data acquired by the laser scanning system provide raw surface points that consist of X, Y, and Z coordinates for each laser footprint. Segmentation of the points is a necessary process to obtain an explicit and meaningful description of the surface. This involves further process such as building reconstruction and modeling, and object recognition (Csathó *et al.*, 1999; Heuel and Kolbe, 2001). The objective of clustering or segmentation in this study is to group the LiDAR point clouds into different surfaces of the buildings from which the laser points reflected. The clustered points were then used to form planar surfaces of the buildings through the least-square fitting process.

The study site selected for this study is a heavily populated urban area with tall apartment buildings (*i.e.*, fifteen to twenty storied buildings), and the average point density was six points per square meter. Fig. 1 shows perspective view of the study area generated by triangulated irregular network (TIN) surface modeling of the LiDAR points. Fig. 2 shows schematic diagram of the major processing steps for clustering LiDAR point clouds and 3D building reconstruction.

This study proposes to utilize gray value coded image of the LiDAR heights and histogram to determine the initial approximations of building boundaries (Fig. 3).

Firstly, histograms of the laser point height were analyzed to divide the point clouds into potential roof

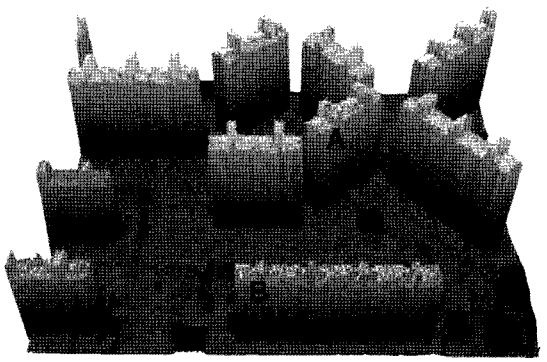

Fig. 1. 3D visualization of part of the LiDAR point clouds. (A and B are test buildings)

points and non-roof points (Fig. 4). The histograms were generated for each building that was composed with laser point clouds located around the building area (see Fig. 7). Then, the roof plane was reconstructed using the LiDAR points within the boundary of the building footprint (Elaksher and Bethel, 2002; Lee, *et al.*, 2002). To extract the building boundaries an edge detection operator was applied to the LiDAR height image. Since distinctive gray level differences occur between ground surface and buildings, different edge detection operators such as Canny, Deriche, and Lanser showed similar results. The building corner points were measured manually on the edge image or the LiDAR height image.

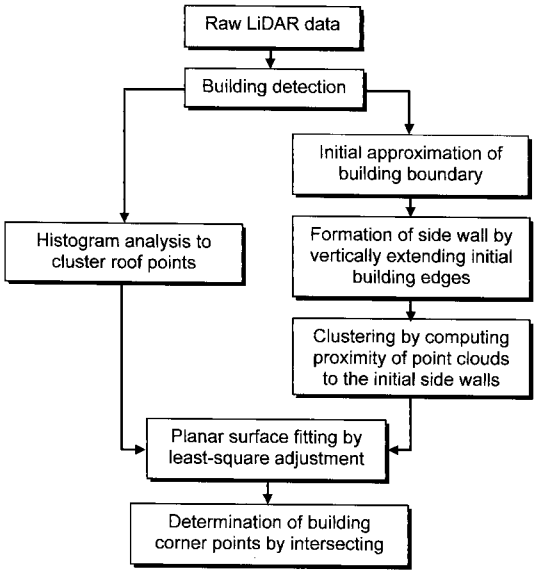

Fig. 2. Schematic diagram of 3D building reconstruction.

2.1 Determination of Initial Building Boundary

The initial boundaries obtained from the edge detection process facilitated the clustering process with efficient handling of the huge volume of points. Each line equation established from two corner points represents an edge of the initial boundaries (Fig. 5). Then the planar equations to depict approximation of the side walls were formed (Fig. 6). The Buffer areas (A, B, C, and D in Fig. 7) were created and only the points within the buffer

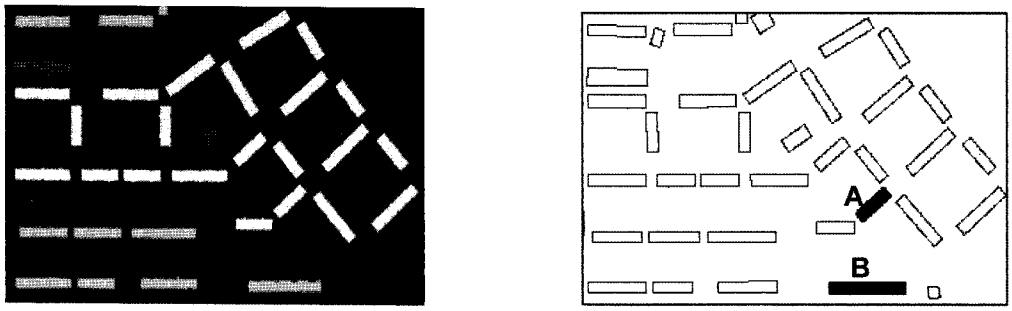

(a) Gray value image of LiDAR heights (b) Extracted buildings

Fig. 3. LiDAR data of study area. (Black rectangles A and B are sample buildings)

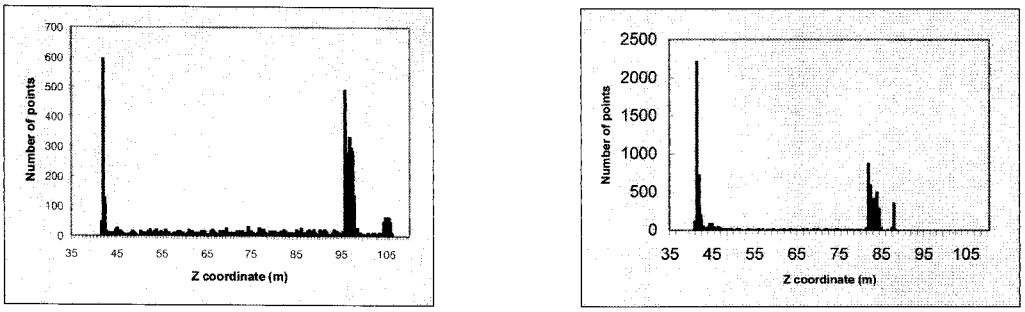

(a) Building "A" (b) Building "B"

Fig. 4. Histogram of the LiDAR elevations. (Left and right peaks represent ground and roof points, respectively)

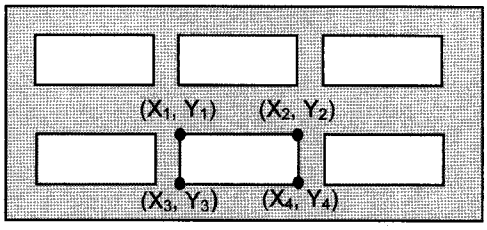

Fig. 5. Building corner coordinates measurements on the extracted buildings.

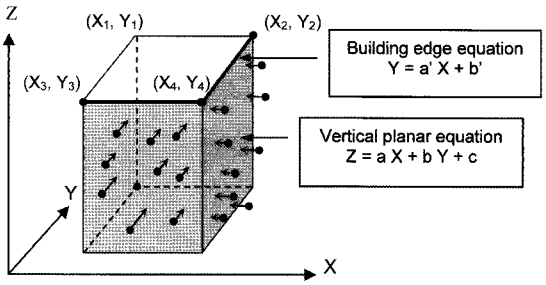

Fig. 6. LiDAR points with normal vectors to the side walls created by extending building edge equations vertically in three-dimensional space.

areas were used in the computation. This results in both efficiency and accuracy improvement.

2.2 Refinement of Initial Building Boundary

The segmentation of the point clouds was performed by computing surface normal distance from the points to the corresponding initial side wall. Surface normal distance between a point (X_i, Y_i, Z_i) to the planar surface, $AX + BY + CZ + D = 0$ is computed as:

$$d_i = \frac{AX_i + BY_i + CZ_i + D}{\sqrt{A^2 + B^2 + C^2}} \quad (1)$$

The points whose distance (d_i) were shorter than a threshold value (*i.e.* 0.6 m in this study by taking density and LiDAR accuracy into account which is around twice of the average distance between laser points.), then the points were assigned to the specific initial side wall. The initial boundaries were then adjusted by least-square surface fitting using clustered points for each side wall (Fig. 8). As the result, five planar surfaces of each building - roof, front, back, left and right side walls were re-

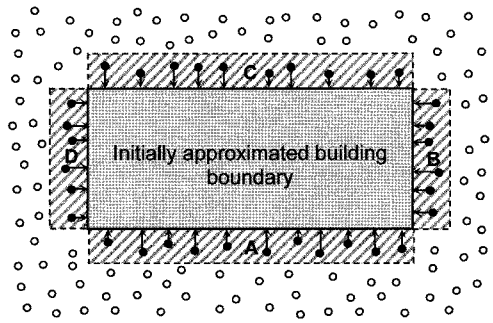

Fig. 7. Buffer areas for computation of the surface normal distance. The initial building boundaries were estimated from LiDAR elevation image. The LiDAR points were segmented into each side wall (A: front, B: right, C: back, D: left) based on the surface distance. (Black dots represent points belong to building wall, white dots represent non-building points such as ground points)

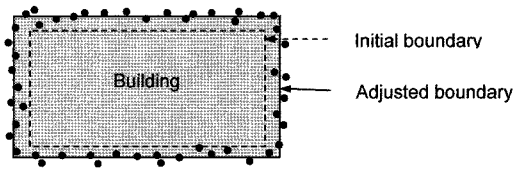

Fig. 8. Initial building boundary (dashed line) and final building boundary from planar surface fitting with least-square method (continuous line).

constructed. Finally, intersection of the surfaces provided boundaries between surfaces and corner point coordinates that are the fundamental information for 3D building reconstruction. Planar surface equation is expressed as:

$$Z = aX + bY + c \quad (2)$$

where a and b represent slope in X and Y direction, respectively, and c denotes intercept. The plane parameters are determined by least-square adjustment:

$$Z = A\xi + e \quad (3)$$

where $Z = \begin{bmatrix} Z_1 \\ Z_2 \\ \dots \\ Z_n \end{bmatrix}$, $A = \begin{bmatrix} X_1 & Y_1 & 1 \\ X_2 & Y_2 & 1 \\ \dots & \dots & \dots \\ X_n & Y_n & 1 \end{bmatrix}$, $\xi = \begin{bmatrix} a \\ b \\ c \end{bmatrix}$, and error

vector: $e = \begin{bmatrix} e_1 \\ e_2 \\ \cdots \\ e_n \end{bmatrix}$

$$\xi = (A^T A)^{-1} A^T Z. \quad (4)$$

Building corner coordinates are computed by intersecting three adjacent planes:

$$x = B^{-1} c \quad (5)$$

where $x = \begin{bmatrix} X \\ Y \\ Z \end{bmatrix}$, $B = \begin{bmatrix} -a_1 & -b_1 & 1 \\ -a_2 & -b_1 & 1 \\ -a3 & -b_1 & 1 \end{bmatrix}$, and $c = \begin{bmatrix} c_1 \\ c_2 \\ c_3 \end{bmatrix}$

The results were compared with a large scale digital topographic map compiled by aerial photographs. National digital vector map with scale of 1/1,000 was used as reference data to evaluate accuracy of the results. However, the map provides planimetric information only, the height accuracy was evaluated by examining the histograms of the LiDAR heights.

3. Roof Shape Analysis

3.1 Accumulated Differential Slope

While most of the side walls of the buildings are vertical plane, roofs have various shapes. Therefore, it is not appropriate for realistic building modeling to fit the roofs with a simple horizontal plane. One would need to initially decide whether a roof consists of a horizontal flat surface or complex surfaces. This can be performed by evaluating the standard deviation of the height values (*i.e.*, Z coordinates) of the LiDAR points. If the standard deviation is larger than a certain value, then most probably the roof is not a horizontal plane. In this case, the RMSE (root mean square error) is also large after least square fitting due to the large residuals (Maas, 2001; Rottensteiner, 2002; Vosselman, 1999).

The proposed scheme in this section aims to reconstruct the roof using a differential slope accumulation method. The concept of implementing accumulated differential slope was derived by extending "*ψ-s curve*" representation of 2D geometric structures, that was introduced by Ballard (1982), to 3D objects. The original *ψ-s curve* represents an object with curvature along the object boundary. The advantage of this method is scale invariant representation of the features. The *ψ-s curve* was modified for this study as: (1) slopes in X-direction and Y-direction for each grid of the roof tops are computed instead of the curvatures, and (2) slope values of each direction are accumulated along the profiles of X-direction and Y-direction as shown Fig. 11. "Differential slope" means that slope for each small grid or slope between sample points.

The shapes of the accumulated differential slopes are similar to the actual roof shape. However, the roof models constructed by accumulated differential slope have scale invariant property. Therefore, more descriptive representation in establishing model database for model-driven approach might be possible. Fig. 9 depicts an example of computing accumulated differential slope for a gable roof. The accumulated differential slope of the each building can be obtained with the same fashion. A differential slope between regularly spaced points and accumulated differential slope are computed by Equation 6 and Equation 7, respectively:

$$dS = \Delta Z / \Delta X \quad (6)$$

$$S = \sum dS \quad (7)$$

where ΔX sample distance of the regular grid, and ΔZ height difference between points. Since each building footprint was determined in the previous procedure, roof shape analysis based on the accumulated differential slope was performed for individual building within the building boundary.

First, the roof types are analyzed based on the slope information. This information will be used to segment roof faces. Consequently, the LiDAR points for each segment are then used to find its surface equation. The intersecting edges of different roof surfaces are then identified and located.

3.2 Identification of Roof Type

We have made six prototypes of roofs as shown in Fig. 10. These synthetic surfaces were generated with maximum random noise of 0.4 m that could depict

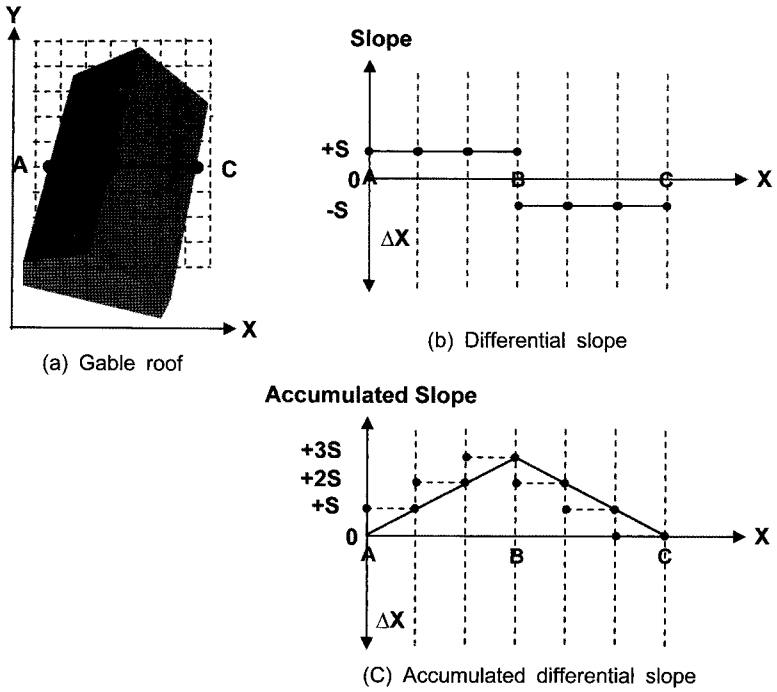

Fig. 9. Accumulated differential slope for a profile (A-B-C) of a gable roof.

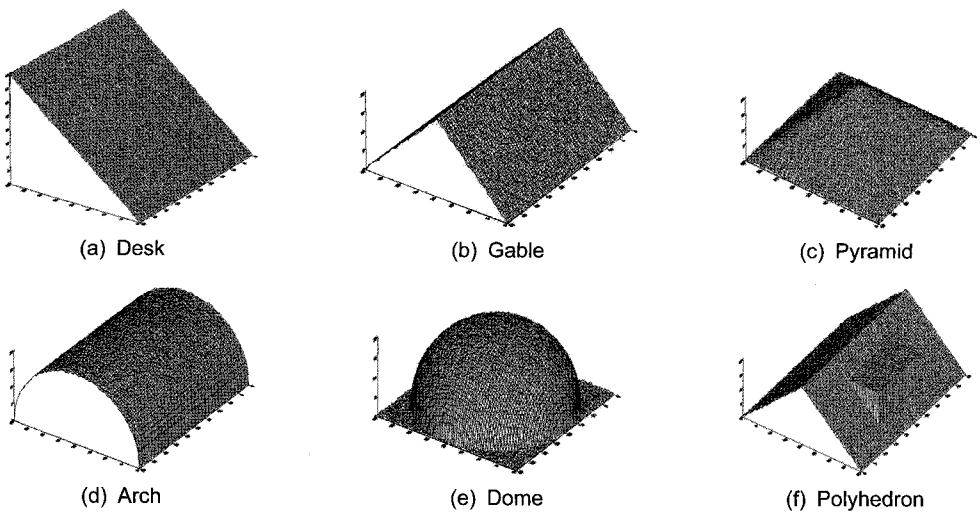

Fig. 10. Typical types of roof structure.

LiDAR data. As can be seen, arched roofs and domes are also included which can be analyzed by the novel approach taken in this study. To identify the roof type, the sporadic LiDAR points were interpolated to the regular grids. Bilinear interpolation was employed in this study. Then the roof profiles were generated along the cross sectional lines (both X and Y directions) of points.

The cross sections were generated by accumulating the slopes between points. Accumulated differential slopes of the various roofs are shown in Fig. 11. The resulting

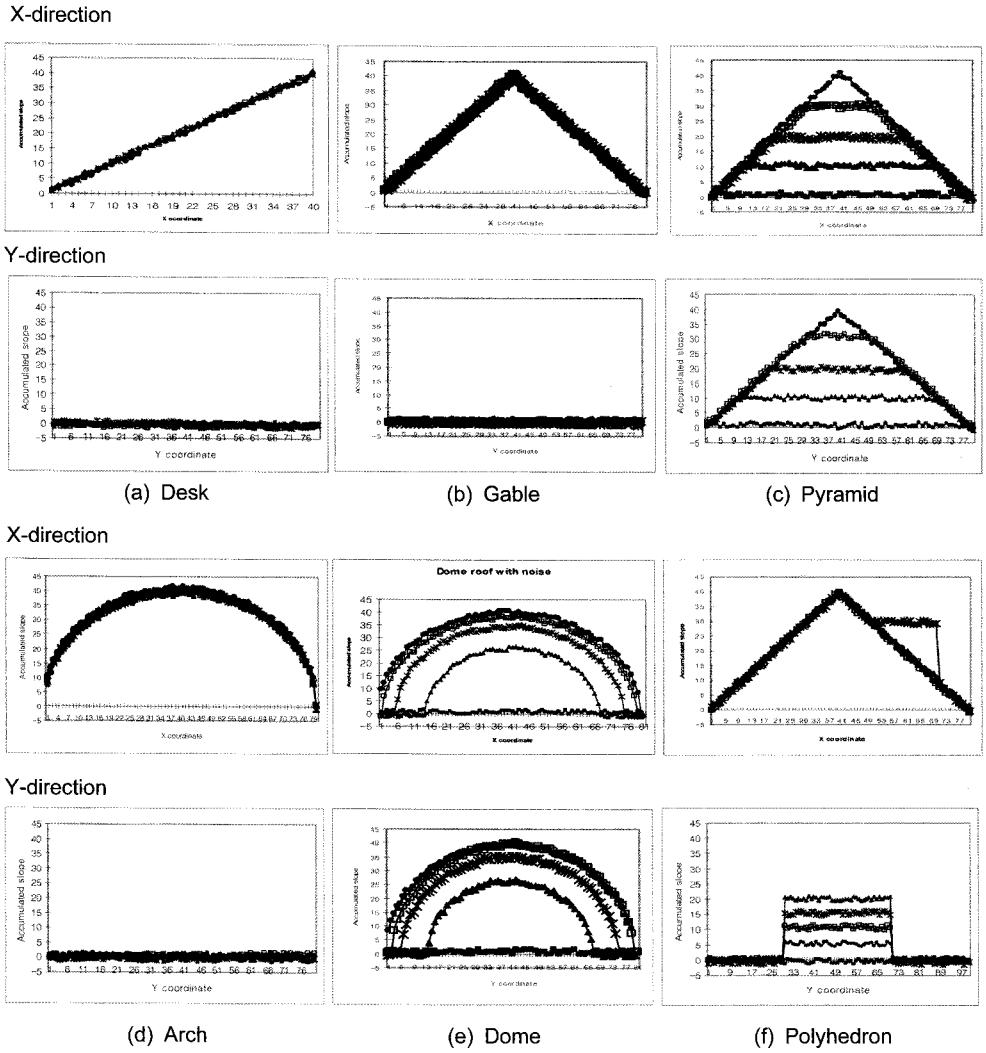

Fig. 11. Accumulated differential slopes for each profile of the roof.

slopes render the original shapes of the roof with scale invariance and represent geometric properties of the roof shape. For each type of roof, different numbers of intersecting edges of surface patches exist at various locations. For example gable roof in Fig. 10 (b), the edge formed by adjacent faces in the roof can be identified where the slope takes a sudden dip and the X-coordinate of this edge is determined from Fig. 11 (b).

In order to locating roof face intersecting edges, positions where slope change occurs are determined for each profile. Laser point clouds insides of the area defined by coordinates that represent edges of adjacent faces and the build boundary determined in the previous procedure are used to determine the each face of the roof structure by least square surface fitting. Fig. 12 illustrates procedure of determining roof surface patches with laser point clouds on the roof planes.

4. Experimental Results and Discussion

LiDAR data was collected by Optech ALTM 3070 system at flying height of 1,200 m. According to the specification of the system, planimetric and vertical accuracy at this height are 0.60 m and 0.15 m, respec-

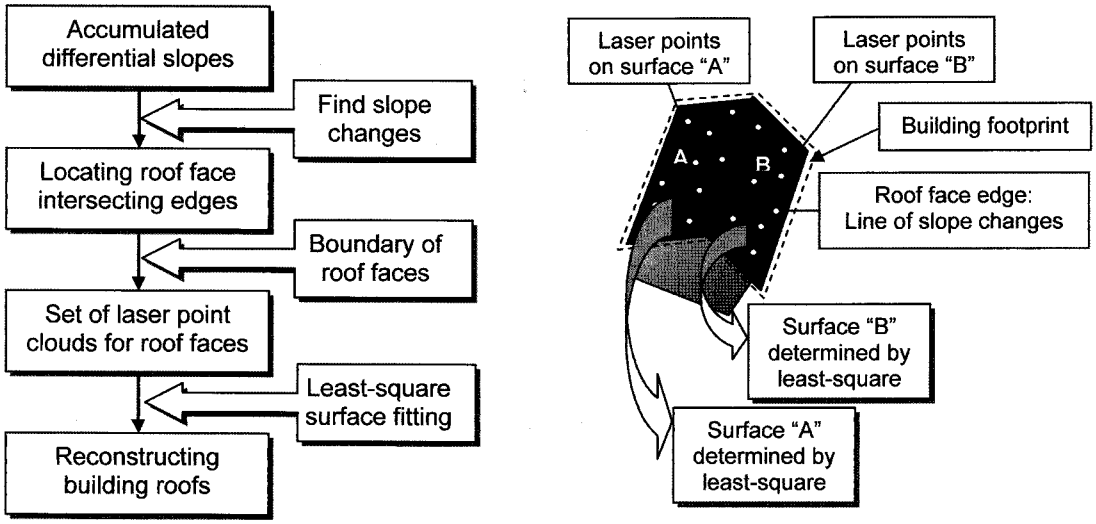

(a) Procedure of roof reconstruction (b) Illustrative description of roof reconstruction

Fig. 12. Roof type analysis and reconstruction.

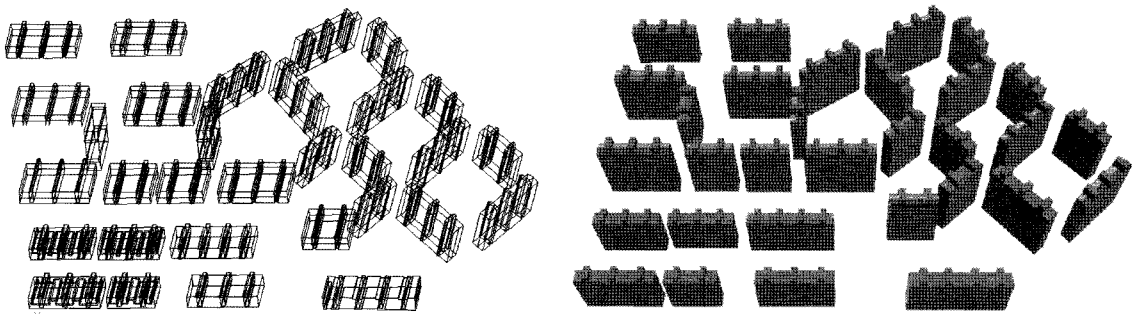

(a) 3D digitized buildings using aerial photos (b) 3D building models using proposed method

Fig. 13. Comparison of 3D building reconstruction.

tively. Fig. 13 shows 3D building models. The four corner coordinates of the reconstructed buildings were compared with the digital vector data. As examples of the results, accuracy of the building "A" and building "B" are shown in Table 1. The planimetric accuracy might satisfy with the accuracy specification of the large scale digital vector maps. 3D building data, which were produced by manual digitizing stereo aerial images on the digital photogrammetric workstation, were utilized to evaluate accuracy of the reconstructed buildings.

The histograms in Fig. 4 show that heights of the building roofs are around 83 m and 96 m for building "A" and building "B", respectively. If other features such as trees are near the buildings, the results would not be as accurate as in this experiment because points from such objects contaminate clustering. The overall accuracies for all thirty one buildings in the study area in terms of RMSEs are around 0.4 m in both X and Y coordinates, and 0.6 m in Z coordinates.

In roof type analysis, corresponding cross sectional accumulated slope diagrams for various cases were generated. For further study, this approach will be developed into fully automatic roof surface generation scheme, and eventually various roof shapes could be represented by most appropriate analytic functions that fit the specific roof structures.

Table 1. Comparison of the results with 3D digital data at corner points. (unit: m)

(1) Building A

Pt.	Digitized data		Proposed method			Difference	
	X	Y	X	Y	Z	dX	dY
1	235291.96	317824.22	235292.02	317824.63	83.00	0.06	0.41
2	235283.57	317833.67	235283.60	317833.20	83.00	0.03	-0.47
3	235314.90	317861.77	235314.70	317861.37	83.00	-0.20	-0.40
4	235323.09	317852.57	235323.17	317852.61	83.00	0.08	0.04
Planimetric error: 0.36							

(2) Building B

Pt.	Digitized data		Proposed method			Difference	
	X	Y	X	Y	Z	dX	dY
1	235255.55	317748.03	235255.71	317748.38	96.50	0.16	0.35
2	235255.62	317761.30	235256.02	317760.98	96.50	0.40	-0.32
3	235339.15	317761.24	235338.63	317760.99	96.50	-0.52	-0.25
4	235339.21	317747.79	235338.76	317748.44	96.50	-0.45	0.65
Planimetric error: 0.57							

5. Conclusions

3D building reconstruction and visualization were performed with airborne LiDAR data in the urban area. Point clouds were clustered efficiently using LiDAR height image and then building surfaces were generated through the least-square method. The method is appropriate for tall buildings because laser point clouds on the side walls of the buildings are utilized. Traditionally the digital vector maps are produced by manual digitizing of images. LiDAR technology has the capability of automatic or semi-automatic generation of the accurate 3D building models and large scale digital mapping. The proposed approach to achieve such aim efficiently satisfied the required accuracy in mapping professions. However, accumulated differential slope of 3D objects is not rotation invariant. Therefore, rotations of the objects with respect to the reference axis are to be determined. One of the limitations of the proposed method is that it requires enough points, and fine features or complex structures of the roof could not be properly modeled.

Using the proposed scheme for roof type analysis, it was possible to obtain cross sectional and geometric information which subsequently will be used to generate planar equations of various roof faces. The promising results with which will enable the reconstruction of complex roof structures using differential slope accumulation method. For further study, it would be recommended to apply appropriate segmentation of the LiDAR data associated with the roof shape analysis.

Acknowledgement

The material presented in this paper is based upon work supported by the Seoul R&BD program (10541).

References

Alharthy, A. and Bethel, J. (2004). Detailed Building Reconstruntion from Airborne Laser Data Using a Moving Surface Method, XXth ISPRS Congress, 12-23 July 2004 Istanbul, Turkey, Commission 3, unpaged CD-ROM.

Ballard D. and Brown, C. (1982). Computer Vision, Prentice-Hall, Englewood Cliffs, NJ., pp. 237.

Chen, L., Teo, T., Shao, Y., Lai, Y., and Rau J. (2004). Fusion of Lidar Data and Optical Imagery for Building Modeling. International Archives of the Photogrammetry, Remote Sensing, Vol. 34, pp. 732-737.

Csathó, B., Boyer, K. and Filin, S. (1999). Segmentation of Laser Surfaces. International Archives of Photogrammetry and Remote Sensing, Vol. 32, pp. 73-80.

Elaksher, A. and Bethel, J. (2002). Reconstructing 3D Buildings from LIDAR Data. Proceedings of Photogrammetric Computer Vision, ISPRS Commission III, Symposium 2002, September 9-13, 2002, Graz, Austria, pp. 102-107.

Flood, M. (1999). Commercial Development of Airborne Laser Altimetry. International Archives of Photogrammetry and Remote Sensing, Vol. 32, pp. 13-20.

Forkuo, E. K. and King, B. (2004). Automatic Fusion of Photogrammetric Imagery and Laser Scanner Point Clouds. International Archives of the Photogrammetry and Remote Sensing, Vol. 34, pp. 921-926.

Forlani, G., Nardinocchi C., Scaioni M. and Zingaretti P. (2003). Building Reconstruction and Visualization from LIDAR Data. The International Archives of the Photogrammetry, Remote Sensing and Spatial Information Sciences, Vol. XXXIV, Part 5/W12, pp. 151-156.

Fowler, R. (2001). Topographic Lidar. In: Digital Elevation Model Technologies and Applications: The DEM Users Manual Maune, D. (ed.): American Society for Photogrammetry and Remote Sensing, Bethesda, MD, pp. 207-236.

Habib, A., Ghanma, M. Morgan, J. and Al-Ruzouq, R. (2005). Photogrammetric and Lidar Data Registration Using Linear Features. Photogrammetric Engineering & Remote Sensing, Vol. 71, No. 6, pp. 699-707.

Habib, A. and Schenk, T. (1999). New Approach for Matching Surfaces from Laser Scanners and Optical sensors. International Archives of Photogrammetry & Remote Sensing, 32 (3W14), pp. 55-61.

Heuel, S. and Kolbe, T. (2001). Building Reconstruction: The Dilemma of Generic Versus Specific Models. KI - Zeitschrift für Künstliche Intelligenz 2001, July, No. 3, pp. 57-62.

Khoshelham K. (2004) Building Extraction from Multiple Data Sources: A Data Fusion Framework for Reconstruction of Generic Models. XXth ISPRS Congress, 12-23 July 2004 Istanbul, Turkey, Commission 3, pp. 980-986.

Lee, D., Yom, J., Kwon, J. and We, G. (2002). 3-Dimensional Building Reconstruction with Airborne LiDAR Data. Korean Journal of Geomatics, Vol. 2, No.2, pp. 33-41.

Lee, I. and Schenk, T. (2001). 3D Perceptual Organization of Laser Altimetry Data. International Archives of Photogrammetry and Remote Sensing, Vol. 34, pp. 57-65.

Maas, H. (2001). The Suitability of Airborne Laser Scanner Data for Automatic 3D Object Reconstruction. Third International Workshop on Automatic Extraction of Man-Made Objects from Aerial and Space Images, 10.-15. june 2001, Ascona, Switzerland.

Maas, H. and Vosselman, G. (1999). Two Algorithms for Extracting Building Models from Raw Laser Altimetry Data. ISPRS Journal of Photogrammetry and Remote Sensing, Vol. 54, No. 2/3, pp. 153-163.

Romano, M. (2004). Innovation in Lidar Processing Technology. Photogrammetric Engineering & Remote Sensing, Vol . 70, pp. 1201-1206.

Rottensteiner, F. and Jansa, J. (2002). Automatic Extraction of Building from LIDAR Data and Aerial Images. International Archives of Photogrammetry and Remote Sensing, Vol. 34, Part 4, pp. 295-301.

Suveg, I. and Vosselman, G. (2000). 3D Reconstruction of Building Models. International Archives of hotogrammetry and Remote Sensing, Vol. 33, part B2, Amsterdam, the Netherlands, pp. 538-545.

Schenk, T. and Csathó, B. (2002). Fusion of Lidar Data and Aerial Imagery for More Complete Surface Description. International Archives of Photogrammetry and Remote Sensing, Vol. 34, pp. 310-317.

Vosselman, G. (1999). Building Reconstruction Using Planar Faces in Very High Density Height Data. International Archives of Photogrammetry and Remote Sensing, Vol. 32, part 3/2W5, Munich, Germany, September 6-10, pp. 87-92.

(접수일 2007. 10. 10, 심사일 2007. 11. 30, 심사완료일 2007. 12. 26)